Journal of Space Safety Engineering 9 (2022) 414–426

Contents lists available at ScienceDirect

Journal of Space Safety Engineering

journal homepage: www.elsevier.com/locate/jsse

The Kinetic casualty risk of uncontrolled re-entries before and after the transition to small satellites and mega-constellations

Carmen Pardini*, Luciano Anselmo

Space Flight Dynamics Laboratory, Institute of Information Science and Technologies (ISTI), National Research Council (CNR), Via G. Moruzzi 1, 56124 Pisa, Italy

ARTICLE INFO

Keywords:
Uncontrolled re-entries
Re-entry risk evaluation
Kinetic casualty risk
Casualty area
Casualty expectancy
Casualty probability

Article history:
Received 13 January 2022
Received in revised form 15 March 2022
Accepted 25 April 2022
Available online 4 May 2022

ABSTRACT

Over the last 11 years (2010–2020), more than 600 intact objects larger than 1 m^2 have re-entered without control into the Earth's atmosphere. The total returned mass was approximately 1100 t, roughly corresponding to the re-entry of nearly 100 t per year, mostly concentrated (79%) in rocket bodies. Objects with a mass greater than 500 kg re-entered every about 8 days, those exceeding 2000 kg every about 2 weeks and those heavier than 5000 kg one or twice per year. The total casualty expectancy associated with uncontrolled re-entries over the past 11 years was of the order of 1.4×10^{-1}, that in 2020 was almost 1.7×10^{-2}, corresponding to a probability of having had at least one victim of approximately 13% and 2%, respectively. Unlike the alert threshold of 10^{-4}, linked to single re-entry events, no cumulative risk limit exists for satellite re-entries over one year or more. However, the casualty probability, although still relatively small, cannot be considered negligible, even in view of the launches of mega-constellations planned in the coming years. For instance, if no design for demise was implemented, the addition of 4000 spacecraft re-entering annually would increase the probability of having at least one victim to nearly 30% per year, while 20,000 more satellites would boost it to almost 80%.

1. Introduction

Space activities are in the midst of an epochal transformation. As of mid-July 2021, more than 11,500 satellites have been launched since the beginning of the space age, in 1957, of which almost 7600 are still in orbit and nearly 4400 functioning. However, in the next decade alone, the launch of another 100,000 satellites is planned, radically changing the modalities and scale of space operations.

The kinetic casualty risk from uncontrolled re-entries will be affected as well. Due to the huge number of new payloads placed in low altitude orbits, or disposed from higher orbits in order to comply with space debris mitigation measures, the number of uncontrolled re-entries will increase accordingly. During the long phase preceding this authentic revolution, characterized by small satellites and mega-constellations, the casualty risk of uncontrolled re-entries was generally managed object by object, for example by evaluating whether or not a single event might result in exceeding a certain casualty expectancy threshold, often set equal to 10^{-4}. But the profound change in space activities we are experiencing may require a shift to a more holistic approach to the problem, at the very least more system-oriented than object-oriented. In fact, as an example, even if a single re-entering satellite of a mega-constellation can have a casualty expectancy equal to $\sim 10^{-5}$, i.e. below the widespread alert threshold of 10^{-4}, if 100 satellites per year re-enter, their overall casualty expectancy becomes equal to $\sim 10^{-3}$, i.e. comparable to, or greater than, that of events, such as the re-entries of UARS [1] or Tiangong-1 [2], which received great international attention.

In order to evaluate the rationale and the need of a new general approach to the casualty risk, this study starts reviewing in detail the uncontrolled re-entries of satellites and rocket bodies occurred during the last 11 years, i.e. the period of time covering the transition from "old space" to "new space economy". Then, using several formulations for estimating the kinetic casualty area or expectancy as a function of the re-entering dry mass, the global evolution of the re-entry risk in the time interval considered is evaluated and discussed. This preliminary analysis is then projected in the near future, taking into account the planned launches, the current operational experience of the first mega-constellations and the envisaged mitigation practices leading to re-entries. The discussion of the results and the consequent proposals finally conclude the analysis.

2. Artificial objects decayed in the Earth's atmosphere

As of 15 July 2021, a total of 3646 payloads, 3993 rocket bodies and 17,880 orbital debris have re-entered in the Earth's atmosphere [3]. Since the beginning of the space age, this corresponded, on average, to the re-entry of 1 intact object (either payload or rocket body) every 3 days, plus the re-entry of 1 piece of debris every 31 h. The associated returning mass, amounting to approximately 33,200 t [4], was mainly

* Corresponding author.
E-mail addresses: carmen.pardini@isti.cnr.it (C. Pardini), luciano.anselmo@isti.cnr.it (L. Anselmo).

https://doi.org/10.1016/j.jsse.2022.04.003

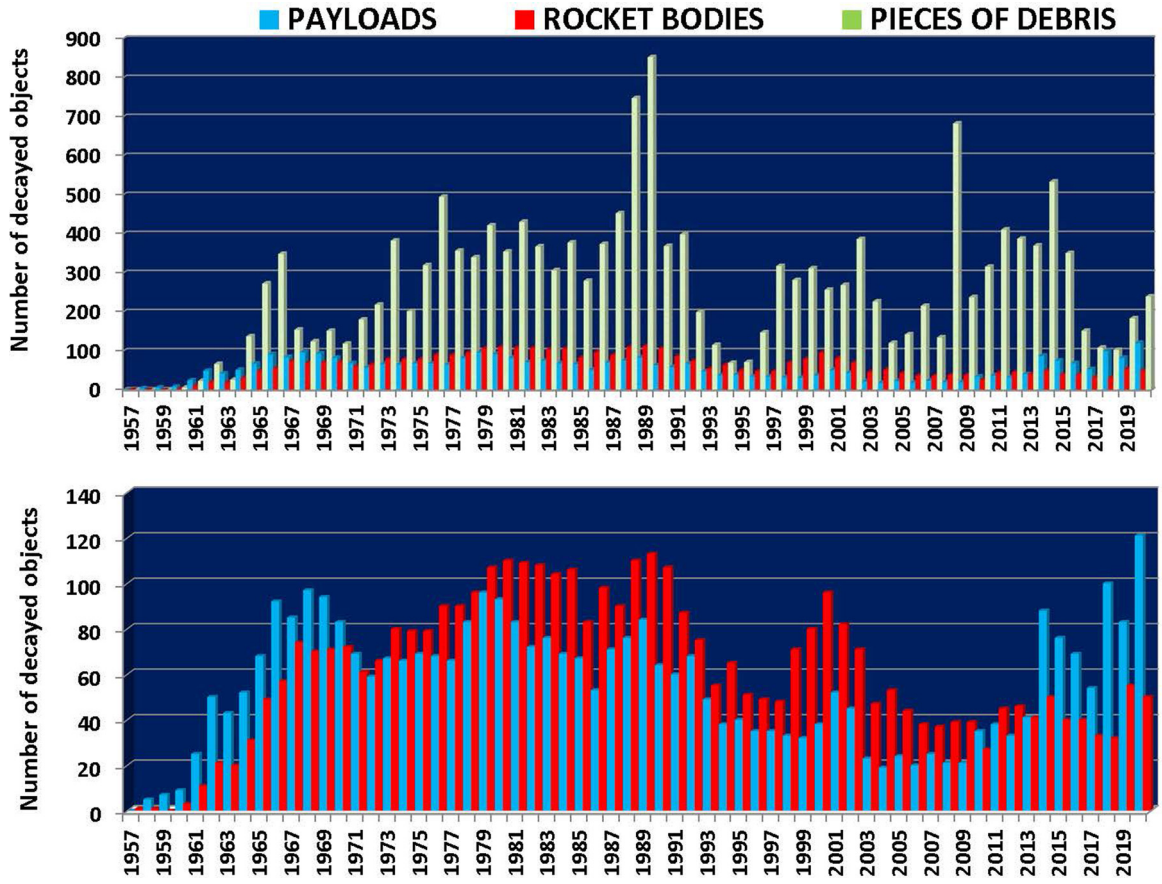

Fig. 1. Re-entries per year of artificial space objects (top) and intact objects (bottom) from the beginning of the space age until the end of 2020 (Data on the re-entered space objects per year were derived from the US Space Track Organization: www.space-track.org).

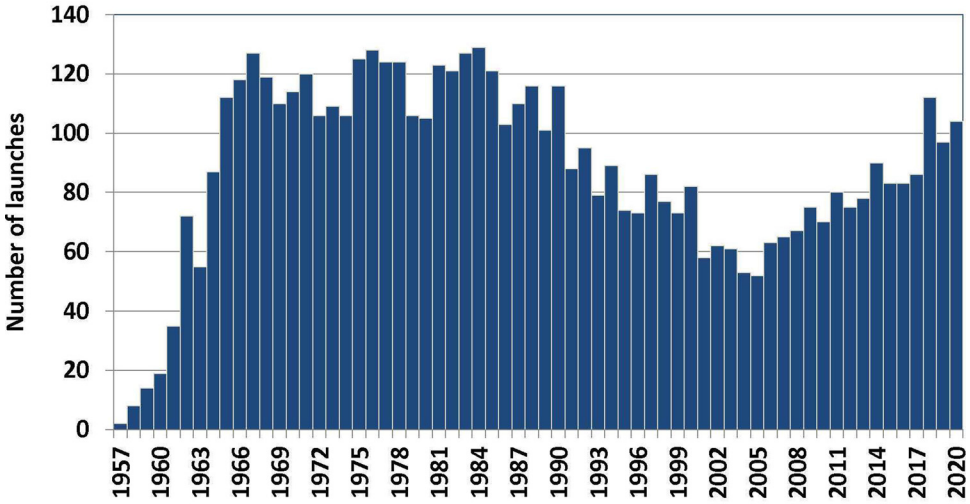

Fig. 2. Orbital launches per year from the beginning of the space age until the end of 2020 (J.C. McDowell, Orbital Launches: https://planet4589.org/space/gcat/data/ldes/O.html).

concentrated (~98%) in intact objects [5]. During the space age, the trend of the re-entries into the Earth's atmosphere (Fig. 1) has been affected by the following factors:

- The rate of launches (Fig. 2), which was influenced by geopolitical, economic and technological aspects (space race, cold war, dissolution of the Soviet Union, constellations, micro-satellites, new space economy);
- The type of missions (operational and parking orbits, ratio between very low, low, medium and geosynchronous Earth orbits);
- On orbit fragmentation events, mainly accidental and unexpected, but also intentional;
- The solar activity (Fig. 3), which, with an 11-year periodicity, significantly increases and decreases the atmospheric density at satellite altitudes, causing drastic changes in the rate of orbital decay and re-entry of objects in low Earth orbit.

2.1. Uncontrolled re-entries during the last 11 years

During the last 11 years, from 1 January 2010 to 31 December 2020, re-entered on average 67 payloads, 42 rocket bodies and 287 debris per

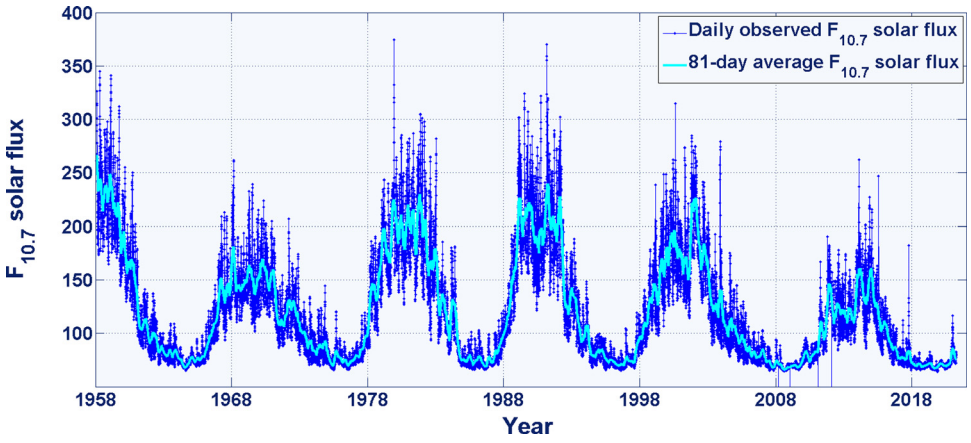

Fig. 3. Solar activity, in terms of the daily observed and 81-day average solar flux at 10.7 cm, $F_{10.7}$, from the beginning of the space age until the end of 2020 (The daily observed solar flux was obtained from NOAA SWPC: https://www.swpc.noaa.gov, and from Jan Alvestad: https://www.solen.info/solar).

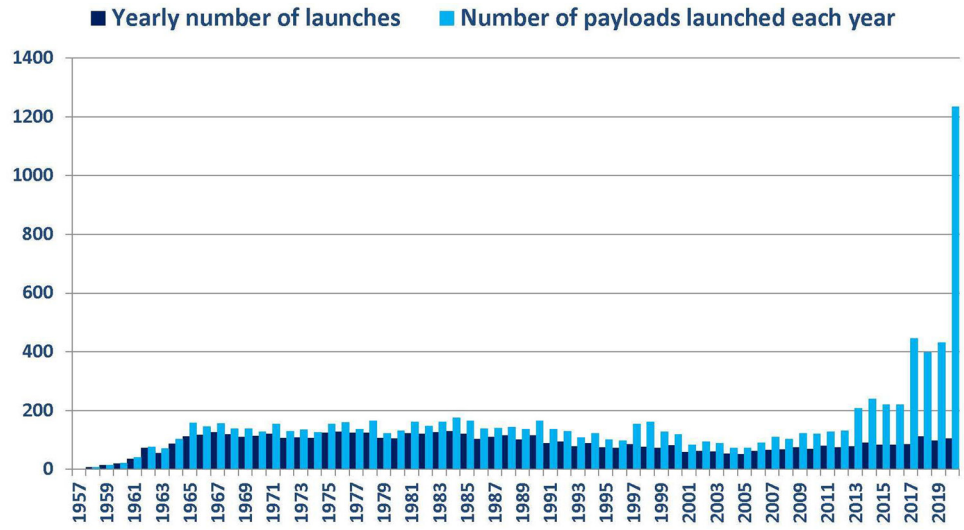

Fig. 4. Yearly number of launches and payloads launched each year since the beginning of the space age, until the end of 2020.

year. In the last 3 years, from 1 January 2018 to 31 December 2020, while the average number of re-entered debris per year decreased by about 39%,[1] compared with the average over the past 11 years, and that of the rocket bodies remained practically the same, there was instead a significant increase – about 51% more than the average over the last 11 years – in the annual decay rate of payloads.

These data are clearly indicative of the changes taking place in space activities, characterized by numerous multiple launches of small satellites (Fig. 4), resulting in an immediate increase in the number of re-entries of the latter compared to that of the other components.

Considering only the uncontrolled re-entries of intact objects, classified as "large" (radar cross section > 1 m^2) by the U.S. Combined Space Operations Center (CSpOC), 214 events involved payloads and 417 rocket bodies, with a total mass of 1113 t, i.e. almost 100 t per year. 97.2% of the mass was concentrated in 491 objects heavier than 500 kg, 23.6% in 270 objects heavier than 2000 kg and 17.8% in 28 objects heavier than 5000 kg. Therefore, based on what was observed during the last 11 years and after a careful analysis to sort out the controlled re-entries, the current situation can be summarized as follows:

- On average, approximately 100 t re-enter in the atmosphere uncontrolled every year;
- Objects with a mass greater than 500 kg re-enter uncontrolled every about 8 days;
- Objects with a mass exceeding 2000 kg re-enter approximately every 2 weeks;
- Objects with a mass greater than 5000 kg re-enter one or twice per year.

The total returned mass is associated for nearly 79% to rocket bodies and for the remaining 21% to payloads (Fig. 5).

3. Re-entry risk evaluation

Specific guidelines and standards to minimize the risk to human life and property on the ground have been defined, over the years, by several space agencies and organizations. During the last decades there has been a growing consensus at the international level in considering a casualty expectancy of 10^{-4} as the risk threshold for an uncontrolled re-entry. The main factors affecting the estimations of the risk of human casualty from uncontrolled re-entries include the number of debris expected to reach the surface of the Earth, the kinetic energy of each surviving fragment and the amount of the world population potentially at risk. A kinetic energy threshold of 15 J is typically adopted as the minimum level for potential injury to an unprotected person, while a probability of fatality of 50% corresponds to a kinetic energy of 103 J [6]. A crucial metric to represent and to evaluate the potential risk from re-entering debris is the so-called total debris casualty area (A_C), which for a re-entry event is the sum of the casualty areas of all the pieces able

[1] The reduction was mainly due to the decreasing number of re-entering debris from the two catastrophic collisions involving Fengyun 1C, in 2007, and Cosmos 2251 – Iridium 33, in 2009.

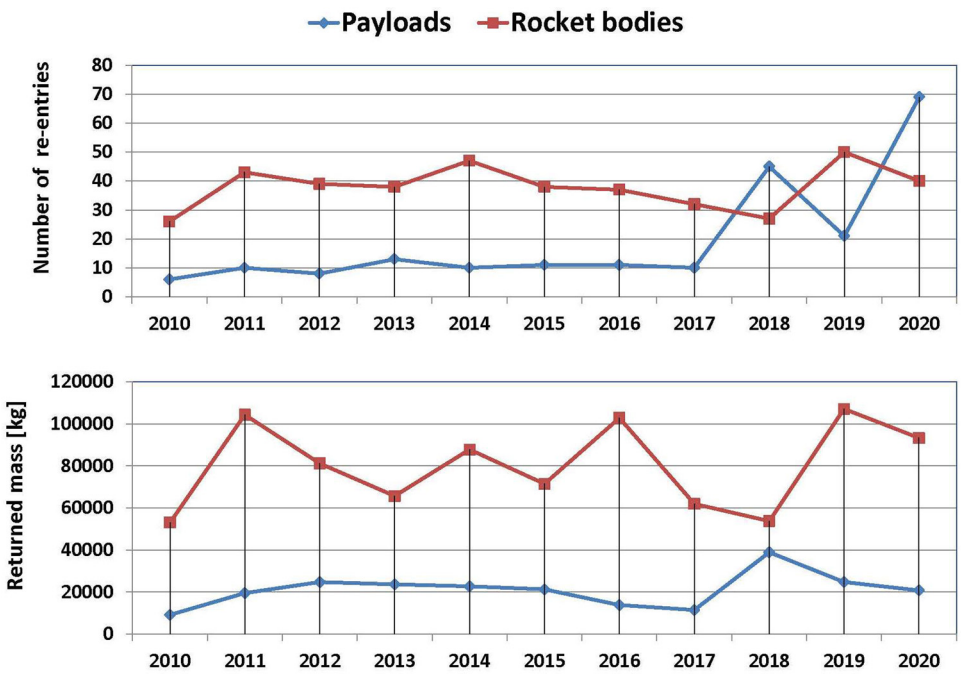

Fig. 5. Yearly re-entries (top) and returned mass (bottom), from 1 January 2010 to 31 December 2020, for payloads and rocket bodies.

to survive the harsh re-entry conditions. It is computed as follow [7]:

$$A_c = \sum_{i=1}^{n} \left(\sqrt{A_h} + \sqrt{A_i} \right)^2 \tag{1}$$

where $A_h = 0.36$ m^2 is the projected cross-sectional area of a standing human and A_i is the cross-section of each individual fragment reaching the ground. A_C is de facto a simple and effective method to combine in a single figure all the information on the breakup process of a re-entering space object, even though Eq. (1) is obviously based on some extremely simplistic hypotheses, as assuming that the whole population is standing and outdoors, that air traffic can be ignored, that the impacting fragments cannot bounce, that if hitting sensitive targets, such as storage tanks for hazardous materials or ground transport systems, secondary casualties cannot be produced, and so on. However, it seems that Eq. (1), coupled with the world-wide population distribution and the orbital inclination of the re-entering object, can still provide the correct order of magnitude of an uncontrolled re-entry risk.

The human casualty expectation, better known as the casualty expectancy (E_C), is obtained as the product of the total debris casualty area (A_C) and the average population density (P_D) in the latitude band overflown by the re-entering object, that is:

$$E_C = A_C \times P_D \tag{2}$$

For instance, a world-wide casualty expectancy of 1:10,000 can be currently reached in a single uncontrolled re-entry event if the total casualty area of the surviving fragments is between 5 and 10 m^2, depending on the orbital inclination of the re-entering objects. For inclinations lower than 20° and higher than 60°, the average population density is lower and a higher total casualty area is needed to obtain a given casualty expectancy, while for intermediate inclinations, between 20° and 60°, the average population density is higher and a total casualty area as small as 5 m^2 may be sufficient to reach the 10^{-4} casualty expectancy threshold.

The re-entry casualty risk can be determined through the probability to cause serious injury or death. For a re-entry event with surviving fragments, and inside the latitude belt overflown by the object, the probability of debris fall is obviously 1, but the expected consequences, at least for people in the open, are not particularly adverse with respect to the common risks accepted in the everyday life. For instance, the risk of being hit by falling orbital debris amounts to about one part per trillion per human per lifetime, i.e. it is of the order of 10^{-12}, that of being hit by a lightning is approximately 1/1500,000, while that of being killed in a car accident amounts to 1/100 in industrialized countries [8].

3.1. Casualty area estimate

Very detailed information on the design and the materials used to build the object under scrutiny is needed to obtain realistic estimates of the casualty area. However, this crucial information is missing in most of the cases and detailed fragmentation analyses are only available for a very limited subset of re-entry events. Therefore, in all cases where this information is not available, it is necessary to resort to alternative, albeit coarser, methods to estimate the casualty area. One possible approach is that described in [9], consisting in deriving A_C from a sample of historical re-entry assessments – carried out with specific software tools for re-entries, such as the NASA's Object Re-entry Survival Analysis Tool (ORSAT) or the ESA's SpaceCraft Atmospheric Re-entry and Aerothermal Break-up software tool (SCARAB) – and then in fitting the results with simple mathematical functions in terms of the re-entering dry mass. For instance, the following linear regression is presented in [9] to relate the casualty area A_C, in m^2, with the dry mass M, in metric tons, of the re-entering object:

$$A_C = 14.58 + 14.49 \times ln(M) \tag{3}$$

Based on the same strategy as in [9], various relationships for A_C were obtained in this paper, starting from the estimate of the casualty area available for a sample of space objects (Table 1), mostly already re-entered. Apart from the PAM-D and Delta 2nd stages, which casualty areas were derived from the recovered fragments, all others casualty areas were estimated using the high-fidelity models SCARAB and ORSAT. Moreover, the casualty areas herein considered were those computed for fragments with impact kinetic energies greater than 15 J.

The distribution of the casualty area A_C as a function of the dry mass M, for the sampled objects, is represented in Fig. 6.

The results shown in Fig. 6 were therefore fitted using the following mathematical functions, where A_C is given in m^2 and M in kg:

Linear (least-squares fitting)

$$A_C = 0.007604M + 2.882 \tag{4}$$

Table 1
Sample of space objects with mass ranging from 230 kg and 14,000 kg, for which the casualty area was available.

Satellite name	Reference*	Satellite mass[kg]	Model to assess the casualty area	Casualty area[m^2]
BeppoSAX Satellite per Astronomia X, "Beppo"	[10]	1385.63	SCARAB	29.816
CGRO Compton Gamma Ray Observatory	[11]	14,000	ORSAT	76.9
Delta 2nd Stage	[12]	800	Estimate based on recovered fragments	10
EUVE Extreme Ultraviolet Explorer	[13]	3243	ORSAT	5.95
HST Hubble Space Telescope	[14]	8844	ORSAT	146
EOS-Aura Earth Observing System-Aura	[15]	2400	ORSAT	10.49
GPM Global Precipitation Measurement spacecraft	[16]	2676	ORSAT	23.38
GLAST/Fermi Gamma-ray Large Area Space Telescope/Fermi	[17]	3639	ORSAT	13.24
GOCE Gravity Field and Steady State Ocean Circulation Explorer	[18]	1034.363	SCARAB	15.675
Iridium (1st generation)	[19]	560	ORSAT	6.1
PAM-D/STAR-48B	[20]	230	Estimate based on recovered fragments	2.8
ROSAT Roentgen (X-ray) Satellite	[21]	2426	SCARAB	31.68
Terra Terra spacecraft	[22]	4427	ORSAT	48.5
Test-sat Generic satellite test case	[21]	400	SCARAB	5.226
TRMM Tropical Rainfall Measuring Mission	[23]	2621	ORSAT	11.3
UARS Upper Atmosphere Research Satellite	[24]	5668	ORSAT	22.38

* Data on the survivability analysis of the object in question can be found in the corresponding reference.

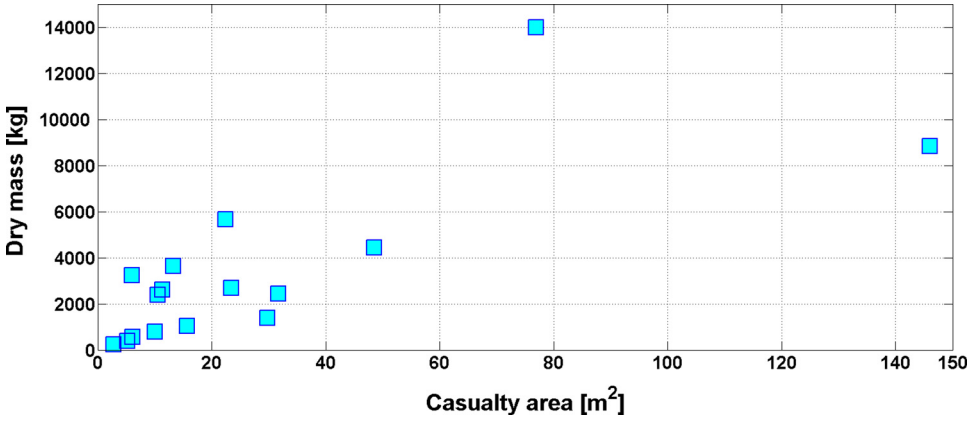

Fig. 6. Casualty area assessment in terms of the dry mass of sampled objects.

Linear (least absolute residuals)

$$A_C = 0.005268M + 3.15 \quad (5)$$

Power (least-squares fitting)

$$A_C = 0.02308M^{0.8834} \quad (6)$$

Power (least absolute residuals)

$$A_C = 0.05627M^{0.7563} \quad (7)$$

Power (bisquare weights):

$$A_C = 0.03351M^{0.8053} \quad (8)$$

3.2. Population evolution

Considering that the population density is proportional, based on Eq. (2), to the expected number of casualties per unit casualty area, the latter was used to represent the evolution of the population. The expected number of casualties per unit casualty area, as a function of the orbit inclination, was kindly provided by A. Kato from JAXA [25]. It is based on the population model GPW4 (Gridded Population of the World version 4, produced by the Center for International Earth Science Information Network, CIESIN) and represents a prospect for 2020 based on data available at the end of 2016. The expected number of casualties per unit casualty area, as a function of the orbit inclination, is shown in Fig. 7 for the year 2020.

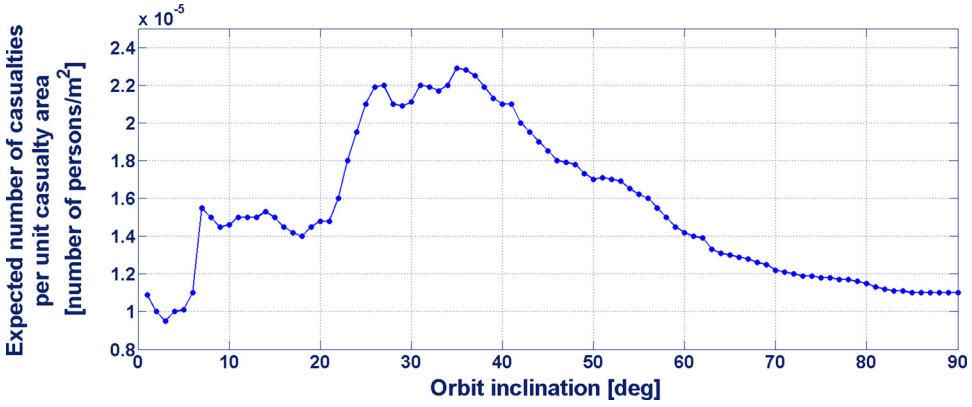

Fig. 7. Expected number of casualties per unit casualty area versus inclination for the year 2020.

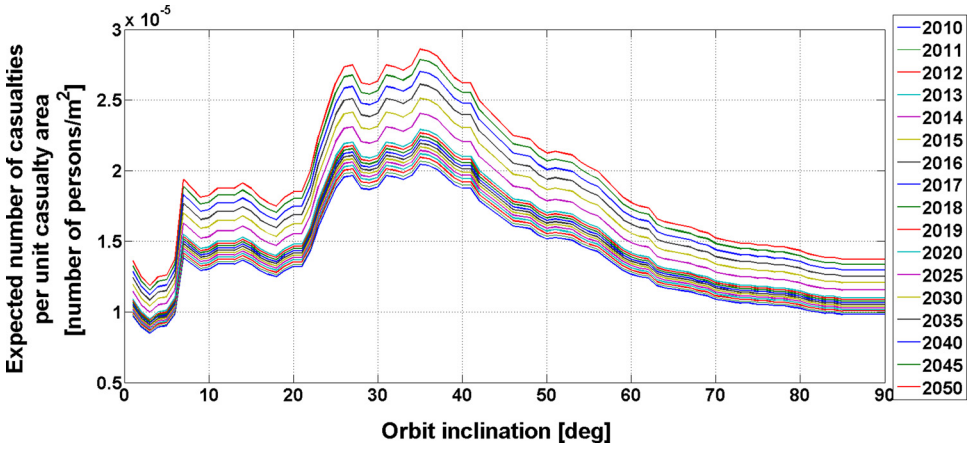

Fig. 8. Expected number of casualties per unit casualty area versus inclination from 2010 to 2050.

Then, considering the world population by year and the population projections [26], yearly percentage decreases and increases were applied to the expected number of casualties per unit casualty area in 2020 to assess the historical expected number of casualties from 2010 to 2020, as well as the projections up to 2050 (Fig. 8).

Finally, for each re-entering object, a rough estimate of the casualty expectancy E_C was obtained by multiplying the object's casualty area (from one of Eqs. (3)–(8) in terms of the dry mass of the re-entering object) by the expected number of casualties per unit casualty area corresponding to the re-entry year and to the orbit inclination of the decaying object.

3.3. ISTI-CNR uncontrolled re-entry magnitude scale definition

Another approach to assess the relevance of uncontrolled re-entries was introduced at ISTI-CNR (formerly CNUCE-CNR) since 1995 [27]. It uses the dry mass M, in kg, of a re-entering object as an indirect indicator of the casualty risk, which is certainly plausible, from a statistical point of view, when the hazard derives from the ground impact of fragments. The magnitude M_R of uncontrolled re-entries was defined as follows [27]:

$$M_R = log_{10}(M/100) \tag{9}$$

This definition was subsequently slightly modified in 2017 as indicated below [3]:

$$M_R = log_{10}(M/100) + 0.3 \tag{10}$$

The order of magnitude of the global casualty expectancy E_C may be then evaluated as:

$$E_C \sim 10^{M_R - 5} \tag{11}$$

4. The kinetic casualty risk of uncontrolled re-entries during the last 11 years

The different approaches just presented for estimating the casualty expectancy were applied to the 631 large intact objects (214 payloads and 417 rocket bodies which, according to the CSpOC classification, are characterized by a radar cross section > 1 m^2) re-entered without control from 1 January 2010 to 31 December 2020, in order to assess their relevance in terms of the potential risk associated with the re-entry. For each of the 8 relationships considered, the number of re-entries was classified per interval of casualty expectancy. These intervals were: $E_C < 0$ (values obtained with Eq. (3) for objects lighter than about 366 kg); $0 < E_C < 10^{-5}$; $10^{-5} < E_C < 10^{-4}$; $10^{-4} < E_C < 10^{-3}$; $E_C > 10^{-3}$. Afterwards, by summing, for each E_C interval, the number of re-entries occurred in all 8 cases, it was found that nearly 65% of the re-entries of large intact objects were characterized by a casualty expectancy between 10^{-4} and 10^{-3}, while about 32% had E_C between 10^{-5} and 10^{-4} (Fig. 9).

Breaking down by type of object, it was found that almost 80% of the rocket bodies had a casualty expectancy between 10^{-4} and 10^{-3}, against 35% of the payloads, while nearly 17% of the stages, against 59% of the payloads, had E_C between 10^{-5} and 10^{-4}. Therefore, in terms of the risk associated with the uncontrolled re-entries of large intact objects occurred over the last 11 years, it can be concluded that almost 65% (80% for upper stages and 35% for payloads) were characterized by a casualty expectancy larger than the alert threshold of 10^{-4}.

4.1. Casualty expectancy and casualty probability for uncontrolled re-entries of large intact objects

The casualty probability $P(k)$, where k is the number of victims, can be obtained from the average number of the expected casualties E_C using

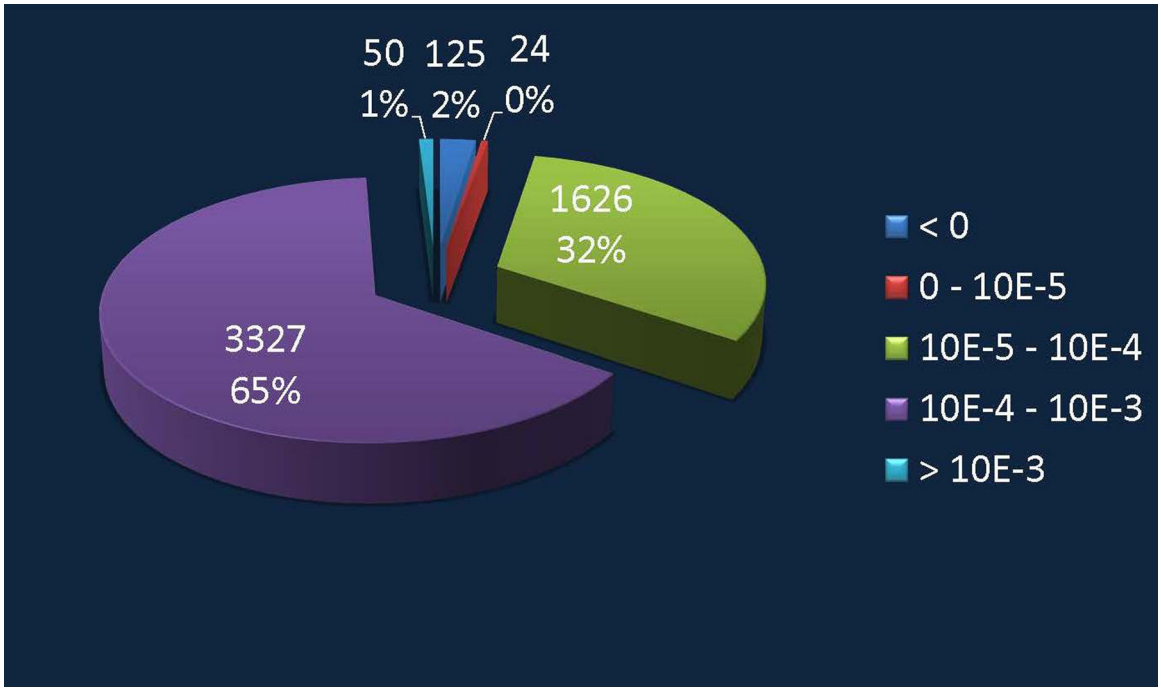

Fig. 9. Distribution, per casualty expectancy interval, of the re-entries of large intact objects occurred from 1 January 2010 to 31 December 2020.

Table 2
Total casualty expectancy per year and probability of having no victims for uncontrolled re-entries of large intact objects occurred between 2010 and 2020.

Year	Total casualty expectancy per year	No casualty probability (%) ($k = 0$)
2010	0.007286	99.27
2011	0.014057	98.60
2012	0.012048	98.80
2013	0.010791	98.93
2014	0.012330	98.77
2015	0.010826	98.92
2016	0.014806	98.53
2017	0.009844	99.02
2018	0.011867	98.82
2019	0.017293	98.29
2020	0.016738	98.34

Table 3
Total casualty expectancy, total casualty area and probability of having no victims for uncontrolled re-entries of large intact objects occurred between 2010 and 2020.

Approach to assess E_C	Total casualty area (m^2)	Total casualty expectancy	Probability of having no victims (%)
Eq. (3)	10,013	0.1437	86.6
Eq. (10)		0.2213	80.2
Eq. (9)		0.1109	89.5
Eq. (4)	10,244	0.1515	85.9
Eq. (5)	7821	0.1153	89.1
Eq. (6)	10,293	0.1522	85.9
Eq. (7)	9389	0.1379	87.1
Eq. (8)	8158	0.1201	88.7
Average*	**9320**	**0.1441**	**86.6**

* The average is over the different approaches used to estimate E_C.

the following Poisson distribution:

$$P(k) = \frac{{E_C}^k \cdot e^{-E_C}}{k!} \tag{12}$$

Herein E_C was estimated by multiplying the expected number of casualties per unit casualty area by the casualty area obtained with Eq. (7). The total casualty expectancy was estimated for each year, from 2010 to 2020, and also for the whole 11-year period.

Table 2 lists the total casualty expectancy per year computed for large intact objects, together with the probability of having no victims ($k = 0$). It was found that, for each year between 2010 and 2020, the probability of having no victims was always higher than 98%, although such value has slightly decreased over the last 3 years. The total casualty area from 2010 to 2020 was more than 9000 m^2 (Table 3), with values in 2019 and 2020 higher by almost 36% and 21%, respectively, with respect to the mean value of the period in question (Fig. 10).

As for the total casualty expectancy per year, Fig. 11 shows an increase of more than 30% over the last two years (2019 and 2020) compared to the 11-year average.

The total casualty expectancy over 11 years, found with Eq. (7), was 0.1379 for large intact objects, corresponding to a probability of having no victims of about 87%, while the probability of having at least one victim was of the order of 13%.

Comparing the results obtained using, in addition to Eq. (7), also Eqs. (3)–(6) and (8) to compute the casualty area, and considering as well Eq. (11), it was found that, over the past 11 years, the total average casualty expectancy due to uncontrolled re-entries of large intact objects was of the order of 0.1441, corresponding to a probability of having no victims of about 87% (Table 3). These average values are in good agreement with those previously obtained using Eq. 7.

The method that differs the most from the others is the ISTI-CNR approach which uses Eq. (10) to assess the magnitude for uncontrolled re-entries. In effect, it overestimated the kinetic casualty risk, with a value of the casualty expectancy which is approximately 53% higher than the average, leading, as a consequence, to a lower probability (~80%) of no victims by re-entering debris in the last 11 years. In general, however, all approaches have shown a very good agreement with each other, with a standard deviation of just 3%.

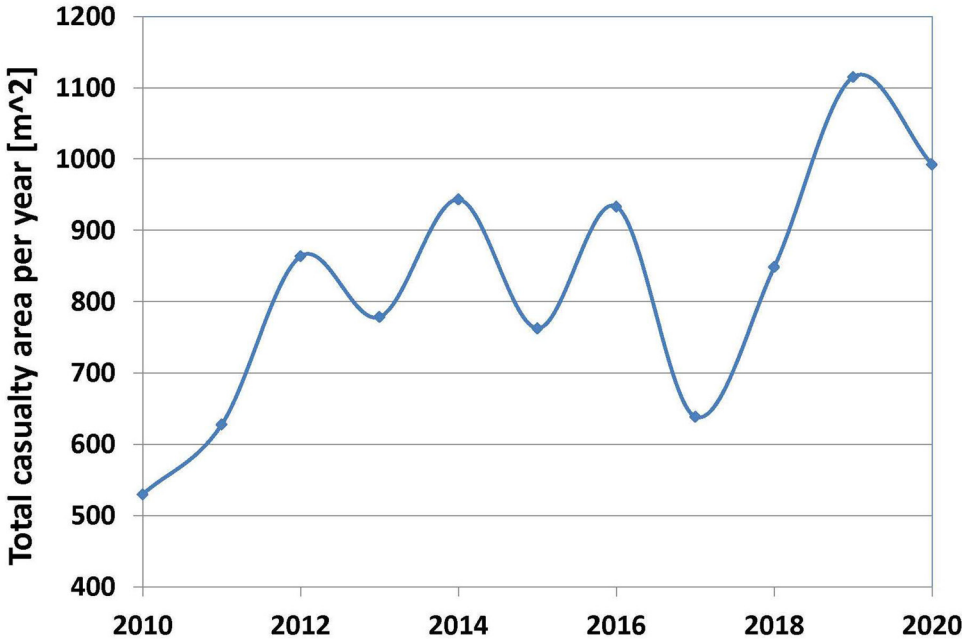

Fig. 10. Total casualty area per year associated to large intact objects re-entered without control between 2010 and 2020.

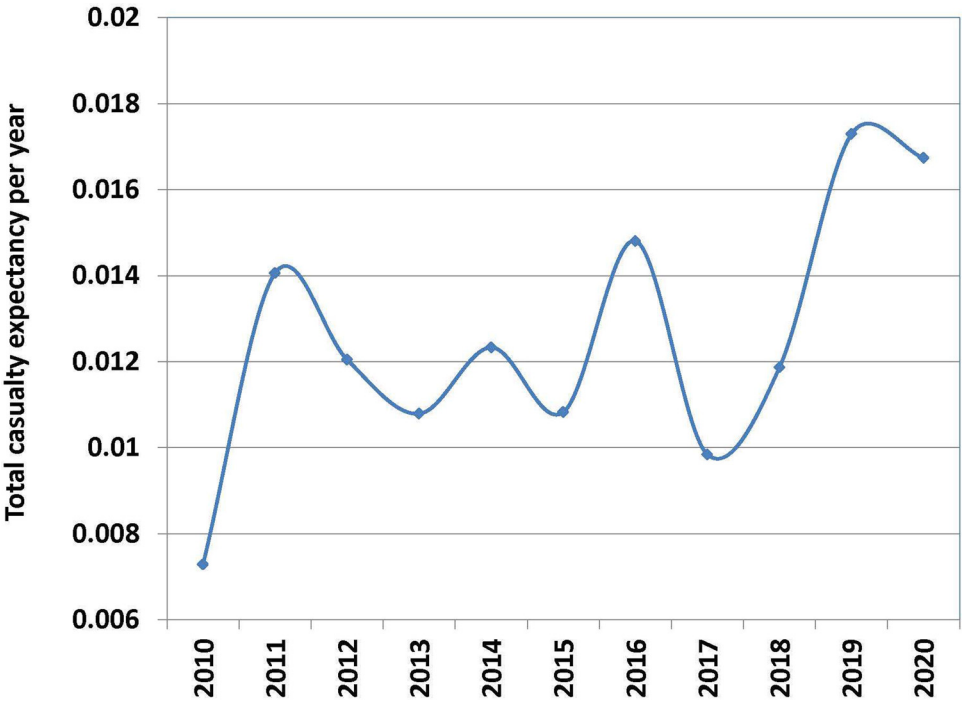

Fig. 11. Total casualty expectancy per year associated to large intact objects re-entered without control between 2010 and 2020.

4.2. Casualty expectancy and casualty probability for uncontrolled re-entries of large payloads

In the 11 years between 2010 and 2020, 214 large payloads have re-entered without control into the Earth's atmosphere. The total casualty expectancy per year, obtained with Eq. (7) to compute the casualty area, is shown in Fig. 12, which, in the last 3 years, highlights a significant increase of E_C due to the decay of numerous satellites from constellations, such as Iridium and Starlink.

The total casualty expectancy over 11 years was of the order of 0.0285, corresponding to a probability of having no victims of approximately 97% and of having at least one victim of nearly 3%. These values were also confirmed by the average over the 8 approaches considered to estimate E_C, as in Table 3. The total casualty expectancy over 11 years is represented in Fig. 13, in terms of the methodology adopted to estimate E_C. Herein, the average value of the casualty expectancy was approximately 0.0286, with a standard deviation around 0.0081 (~28%).

4.3. Casualty expectancy and casualty probability for uncontrolled re-entries of large rocket bodies

In the 11 years between 2010 and 2020, 417 large rocket bodies have re-entered without control into the Earth's atmosphere. The total casualty expectancy per year, obtained with Eq. (7) to compute the casualty area, is shown in Fig. 14, where, differently from payloads (Fig. 12), there was not a significant increase over the last 3 years. The total casu-

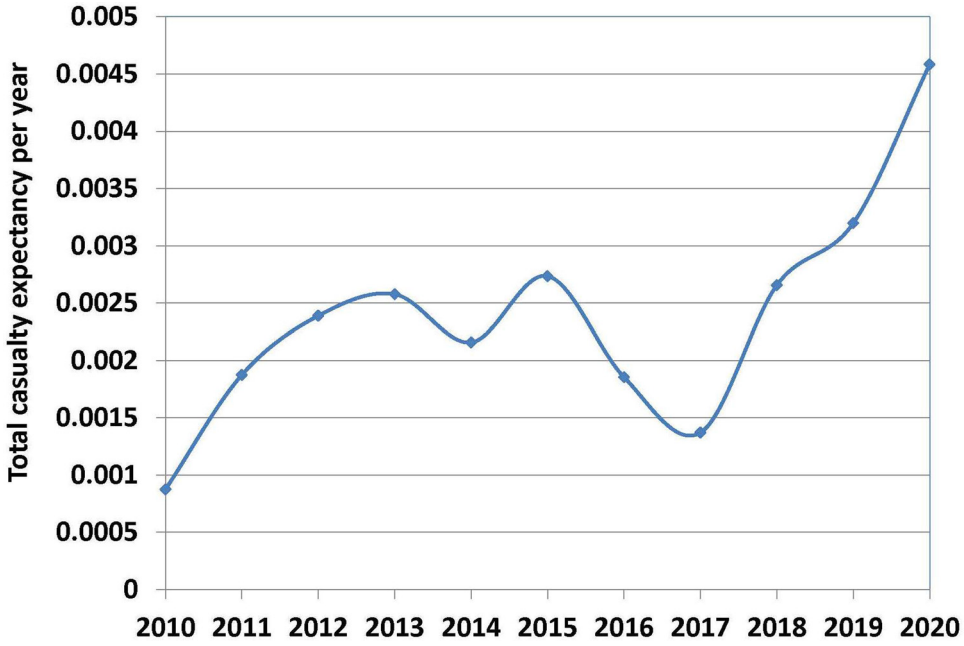

Fig. 12. Total casualty expectancy per year associated to large payloads re-entered without control between 2010 and 2020.

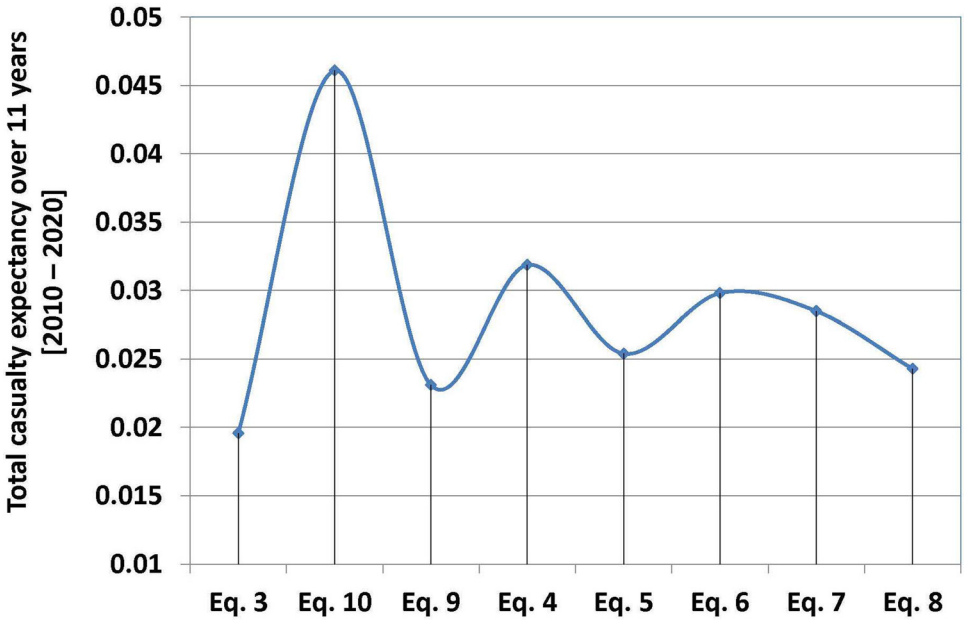

Fig. 13. Total casualty expectancy for large payloads re-entered without control between 2010 and 2020, in terms of the approach used to compute E_C.

alty expectancy over 11 years was of the order of 0.1094, corresponding to a probability of having no victims of approximately 90% and of having at least one victim of nearly 10%. As in previous cases, these values were compared with those resulting from the average of the eight approaches considered to estimate the casualty expectancy (Fig. 15). The average E_C from Fig. 15 was around 0.1155, with a standard deviation of 0.0282 (~24%).

5. Projections of the kinetic casualty risk

In recent years there was a dramatic increase in the launch rate of small satellites in low LEO (Low Earth Orbit). The most impressive development at the moment concerns the deployment of mega-constellations of satellites, with more than 10,000 spacecraft planned in low LEO in the coming years. For instance, the U.S. aerospace company SpaceX has approval from the Federal Communication Commission (FCC) to operate nearly 12,000 Starlink satellites in low LEO – between approximately 340 km and 570 km – with a possible later extension to 42,000, also considering higher altitudes. In late July 2020, FCC approved Amazon's plans to launch 3236 satellites for its Kuiper constellation at altitudes around 600 km. A new Chinese company, named GW, has filed a spectrum application with the International Telecommunication Union (ITU) for two constellations: GW-59 and GW-2, operating below 650 km (GW-59) and around 1145 km (GW-2). With 12,992 communication satellites in orbit, ranging in altitude from 508 to 1145 km and from 30° to 85° in inclination, the Chinese company seems to be interested in the global market, where it would compete with SpaceX and OneWeb. Eventually, if in addition to the already operating constellations, the upcoming and proposed ones are considered, the total number of spacecraft below 650 km might reach values ranging between 10,000 and 50,000 within the next decade. Considering that constellation satellites will be periodically replaced, and that satellites at the end-of-life

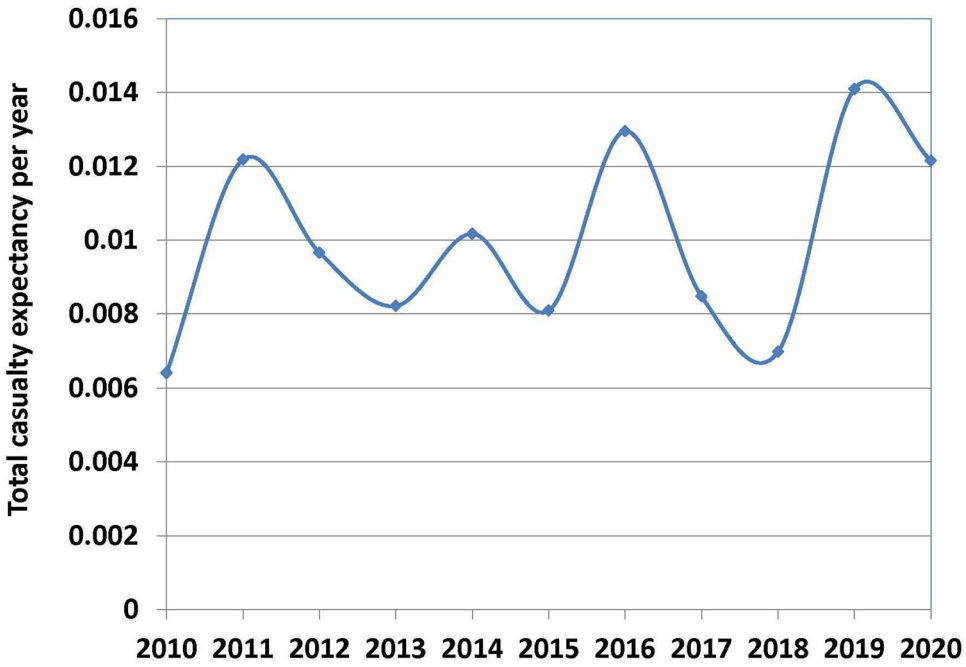

Fig. 14. Total casualty expectancy per year associated to large rocket bodies re-entered without control between 2010 and 2020.

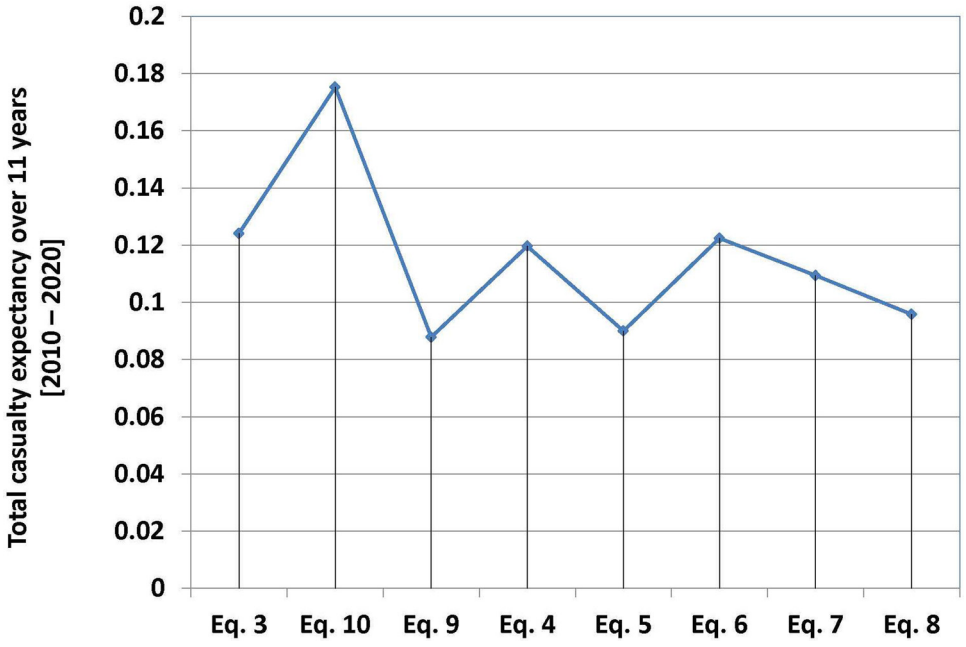

Fig. 15. Total casualty expectancy for large rocket bodies re-entered without control between 2010 and 2020, in terms of the approach used to compute E_C.

will re-enter without control in the atmosphere, we will have to expect a noticeable increase of uncontrolled re-entries of small satellites in the coming years. Taking as an example the Starlink constellation, of which 1656 satellites are currently (6 July 2021) in orbit, of the 1738 satellites launched (excluding the two Tintin), since 24 May 2019, 82 have already re-entered (61 in 2020 and 21 in 2021). Therefore, focusing on what happened in 2020, even if the casualty expectancy associated to a Starlink satellite, with a mass of 260 kg, is of the order of 6.3×10^{-5} (using Eq. (7) to compute the casualty area, equal to 3.77 m^2, and assuming no design for demise), the total casualty expectancy for the 61 re-entries, occurred in 2020, is 3.8×10^{-3}, that is about 83% of the total casualty expectancy for payloads re-entered in 2020 (Fig. 12), and nearly 23% of that for intact objects decayed in 2020 (Fig. 11). It is therefore evident that the launch of thousands of constellation satellites in low LEO will have a far from negligible impact, significantly increasing the global risk due to uncontrolled re-entries, if no design for demise techniques are applied.

Moreover, the low LEO zone will also be significantly affected by the evolution of space activities above this region, because mega-constellations are planned at higher altitudes as well, and in order to mitigate the long-term accumulation of objects and the production of new collisional debris in high LEO, constellation satellites are disposed at the end-of-life to guarantee their relatively fast re-entry in the atmosphere. Therefore, also these satellites will contribute to increase the number of uncontrolled re-entries and, consequently, the re-entry risk.

Making an accurate forecast of what will happen in the near future is practically impossible, due to frequent and sudden changes in the planning of new space activities. However, it was possible to roughly estimate how much the current re-entry risk could increase due to the uncontrolled re-entry of a variable number of satellites not designed for

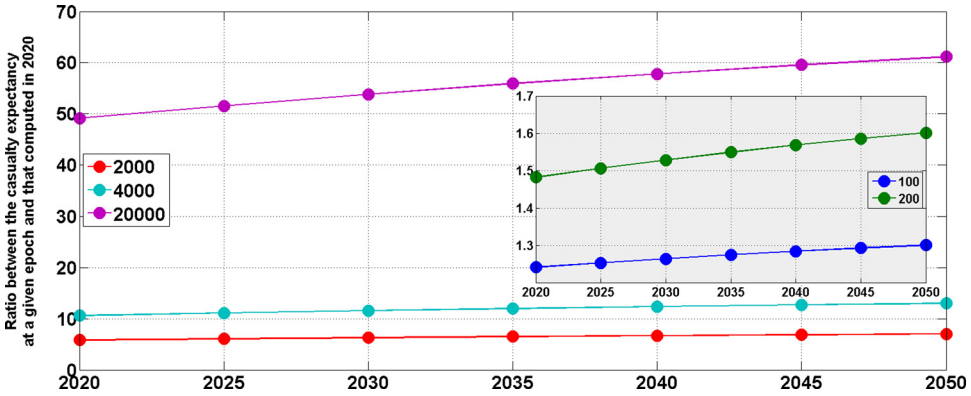

Fig. 16. Evolution of the ratio between the casualty expectancy at a given epoch and that computed in 2020 for 100, 200, 2000, 4000 and 20,000 additional constellation satellites decaying from an orbit inclined by 90°.

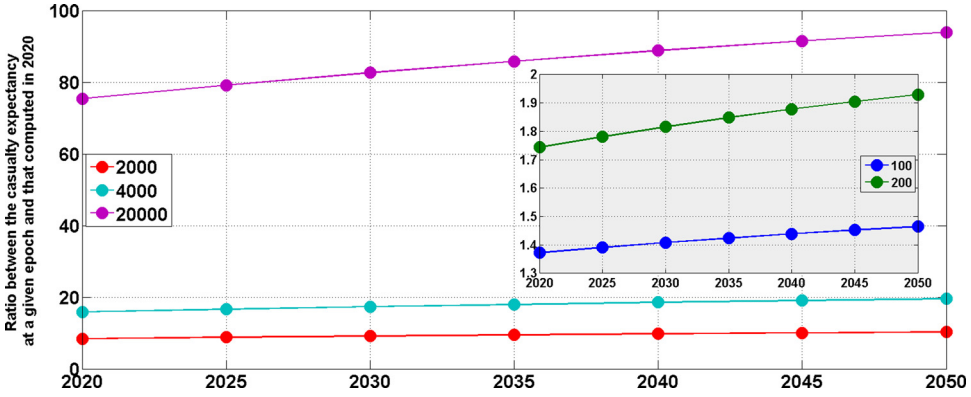

Fig. 17. Evolution of the ratio between the casualty expectancy at a given epoch and that computed in 2020 for 100, 200, 2000, 4000 and 20,000 additional constellation satellites decaying from an orbit inclined by 50°.

Table 4
Casualty expectancy for each single satellite as a function of the orbit inclination and epoch.

Epoch	Orbit inclination		
	35°	50°	90°
2020	8.39E-05	6.23E-05	4.03E-05
2025	8.81E-05	6.54E-05	4.23E-05
2030	9.20E-05	6.83E-05	4.42E-05
2035	9.56E-05	7.10E-05	4.59E-05
2040	9.90E-05	7.35E-05	4.75E-05
2045	0.000102	7.57E-05	4.90E-05
2050	0.000105	7.78E-05	5.03E-05

demise. To give an example, typical small constellation satellites with a mass of 250 kg were considered. Their individual casualty area, computed with Eq. (7), was approximately 3.66 m^2. These satellites were supposed to decay from different orbit inclinations, nearly corresponding to the maximum (35°), medium (50°) and minimum (90°) of the world population density distribution. The number of re-entering satellites per year was assumed to vary from 100 to 20,000, i.e. 100, 200, 2000, 4000 and 20,000. The reference value of the casualty expectancy was that associated with the uncontrolled re-entries of large intact objects in 2020, which was approximately 0.0167 (Fig. 11). Successively, by taking into account the increase of the world population in the next three decades (Fig. 8), projections of the re-entry risk up to 2050 were carried out.

The casualty expectancy for each single satellite – supposed to be a function of the satellite's dry mass, being no more precise information on the demise process available – is represented in Table 4, in terms of the epoch and orbit inclination. Each value of the casualty expectancy was then multiplied by the number of constellation satellites re-entering annually and added to the unrelated re-entry background (assumed to remain constant since 2020) to obtain the corresponding total casualty expectancy for each case. Finally, the ratio between the total casualty expectancy obtained in each case and the reference value in 2020 was computed.

Figs. 16–18 show the evolution of this ratio for 100, 200, 2000, 4000 and 20,000 satellites decaying from orbits inclined by 90°, 50° and 35°, respectively.

Based on the results obtained, the worst scenario occurs when 20,000 satellites re-enter annually from orbits inclined by 35° (Fig. 18). If this were the case, the casualty expectancy would already be 100 times higher than in 2020, and a further increase of the order of 25% would be recorded by 2050, considering the growth trend of the world population. This situation cannot be considered unrealistic at all, since it would roughly correspond to a total of 100,000 satellites put into orbit, with a replacement time of approximately 5 years. But also considering just 3 constellations, such as, for example, Starlink, with 11,926 satellites below 570 km, GW-59, with 6080 satellites below 650 km, and Kuiper, with 3236 satellites below 630 km, the number of satellites in orbit at the same time would be greater than 20,000. Then, assuming again an average lifetime of nearly 5 years, an average of about 4000 satellites would re-enter each year, increasing by about 10–20 times – depending on the orbit inclination – the total casualty expectancy estimated in 2020 (Figs. 16-18).

Concerning the yearly probability of nobody being hit, this would drop from 98.3% (see Table 1 for 2020) to 18.4% if 20,000 more satellites were re-entering as well, passing from 97.5%, 96.7%, 83.1%, 70.3% for 100, 200, 2000 and 4000 additional re-entries, respectively.

It is therefore evident that the launch of mega-constellations in low LEO, together with the disposal of satellites from higher orbits, will entail a significant increase of the kinetic casualty risk in the coming years, if satellites are not designed for demise during re-entry. In fact, even if the value of the casualty expectancy associated with each satellite is below the alert threshold of 10^{-4}, the re-entry of numerous satellites of this type every year could lead to unacceptable values of the associated re-entry risk, both on the ground and in the airspace.

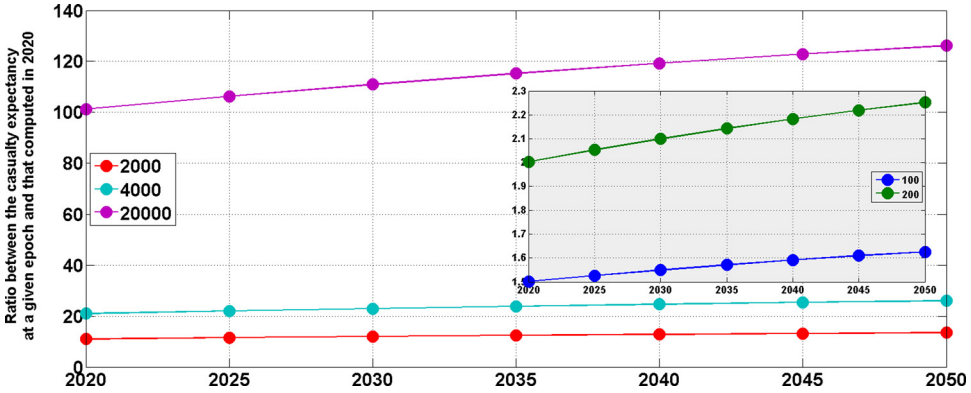

Fig. 18. Evolution of the ratio between the casualty expectancy at a given epoch and that computed in 2020 for 100, 200, 2000, 4000 and 20,000 additional constellation satellites decaying from an orbit inclined by 35°.

The U.S. Government Orbital Debris Mitigation Standard Practices (ODMSP) [28] specify that for large constellations (consisting of 100 or more operational spacecraft), the preferred post mission disposal option is "Direct reentry or heliocentric, Earth-escape". The ODMSP also states that: "In developing the mission profile, the program should limit the cumulative reentry human casualty risk from the constellation". However, no cumulative risk limit has been established for spacecraft re-entries. To cope with this problem, W.H. Ailor of the Aerospace Corporation suggested using the Range Commanders Council (RCC) document RCC 321 [29] as a guidance on how that risk might be managed [19,30]. Concerning acceptable risk criteria for the General Public (GP), the RCC document states that the collective risk for the GP must not exceed a casualty expectancy of 10^{-4} for any single mission. If the annual risk is measured, collective risk for the GP should not exceed a casualty expectation of 3×10^{-3} on an annual basis. Applying this annual limit to each satellite constellation or space system as a whole, as proposed by Ailor [30], could be a reasonable step in the right direction. However, according to the flight and re-entry record, the Starlink mega-constellation, for example, would have already marginally exceeded the proposed ceiling in 2020, if no design for demise was implemented. For this reason, in order to minimize the risk due to surviving fragments, the SpaceX Company is in the process to refine its satellites' components to maximize the probability of them burning up on re-entry.

6. Conclusions

We are going through a period of transition concerning the evolution of space activities. The number of operational satellites in orbit could increase by a factor 10–20 in the coming decades due to the launch of mega-constellations. Furthermore, the application of mitigation measures, to avoid the accumulation of satellites in certain orbital regions in order to reduce the collision risk, would lead to deorbit these satellites at the end-of-life, significantly increasing the number of uncontrolled re-entries into the Earth's atmosphere. Therefore, even if the risk related to uncontrolled re-entries is still relatively low compared to all other risks faced in everyday life, this risk could increase dramatically over the next few years.

The analysis based on the last 11 years, i.e. the time period preceding and partially overlapping such transition phase, confirms that the global casualty probability is still quite low, of the order of less than 2% per year. However, if another 4000 or 20,000 satellites were to re-enter without control every year with no design for demise, the probability of having at least one casualty would become about 30% and 80%, respectively, probably reaching unacceptable values for safety on the ground and in airspace.

In order to minimize such risk, the components of a satellite should be designed and made of materials able to maximize the probability of being burned upon re-entry into the atmosphere. Also SpaceX promised to further revise the components of its satellites and to collaborate with NASA on specific designs that would minimize the risk of hitting people.

However, also this strategy might not be the most appropriate over relatively long periods of time and for thousands of re-entering objects. The problem, in this case, would be due to the release, in the upper atmosphere, of large quantities of chemical substances, like aluminum, that could damage the protective ozone layer. Another effect of the burning of aluminum is the production of aluminum oxide which reflects light at certain wavelengths and, if created in large quantities, may also change the albedo of the planet.

In order to avoid the release of substances harmful to the atmosphere, the satellite should not disintegrate upon re-entry, but in this case it would be necessary for the re-entry to take place in a controlled way to minimize the casualty risk. There is therefore no simple way to address this issue, but it will still be essential that these problems are well analyzed and discussed to avoid running into an irreversible situation, where the re-entry risk is at that point too high to be controlled.

Declarations of Interest

The authors declare that they have no known competing financial interests or personal relationships that could have appeared to influence the work reported in this paper.

CRediT authorship contribution statement

Carmen Pardini: Conceptualization, Software, Formal analysis, Data curation, Writing – review & editing, Project administration. **Luciano Anselmo:** Conceptualization, Writing – review & editing.

Acknowledgements

Part of the work was carried out in the framework of the ASI-INAF agreement No. 2020–6-HH.0 on "Space Debris: support to IADC and SST activities". The authors would also like to thank the U.S. Space Track Organization for making available the catalog of the unclassified objects tracked around the Earth by the U.S. Space Surveillance Network. For data on spacecraft and orbital stages, in particular for their mass, the authors are also indebted to the European Space Agency (ESA) DISCOS Database.

References

[1] L. Anselmo, C. Pardini, Satellite reentry predictions for the Italian civil protection authorities, Acta Astronaut 87 (2013) 163–181, doi:10.1016/j.actaastro.2013.02.004.
[2] C. Pardini, L. Anselmo, Monitoring the orbital decay of the Chinese space station tiangong-1 from the loss of control until the *re*-entry into the Earth's atmosphere, J. Space Safety Eng. 6 (2019) 265–275, doi:10.1016/j.jsse.2019.10.004.
[3] Space-Track.Org. https://www.space-track.org, 2021 (accessed 15 July 2021).
[4] ESA's re-entry prediction. https://reentry.esoc.esa.int/home/history, 2021 (accessed 15 July 2021).

[5] C. Pardini, L. Anselmo, Uncontrolled re-entries of spacecraft and rocket bodies: a statistical overview over the last decade, J. Space Safety Eng. 6 (2019) 30–47, doi:10.1016/j.jsse.2019.02.001.
[6] J.K. Cole, L.W. Young, T. Jordan-Culler, Hazards of Falling Debris to People, Aircraft, and Watercraft, Sandia Report SAND97-0805-UC-706, Sandia National Laboratories, Albuquerque (NM), USA, 1997.
[7] NASAProcess For Limiting Orbital Debris, NASA-STD-8719.14B, NASA Technical Standard,, National Aeronautics and Space Administration, Washington (D.C.), USA, 2019.
[8] C. Nicollier, V. Gauss (Eds.), Our Space Environment: Opportunities, Stakes and Dangers, EPFL Press, Lausanne, Switzerland, 2015.
[9] S. Lemmens, Order of Magnitude Analysis for On-ground Casualty Area from Uncontrolled *Re*-entries, ESA Memo GEN-REN-MO-00228-OPS-GR, European Space Operations Center, ESA, Darmstadt, Germany, 2018.
[10] T. Lips, BeppoSAX *Re*-entry Analysis With SCARAB, HTG-Report-02-8, Hyperschall Technologie Göttingen, Katlenburg-Lindau, Germany, 2002 30 September.
[11] M. Ahmed, D. Mangus, P. Burch, Risk Management Approach for De-orbiting of the Compton Gamma Ray Observatory, in: Proceedings of the Third European Conference on Space Debris, Darmstadt, Germany, 19 - 21 March 2001, ESA SP-473, 2001, pp. 495–500.
[12] W. Botha, Orbital debris: a case study of an impact event in South Africa, in: Proceedings of the Third European Conference on Space Debris, Darmstadt, Germany, 19 - 21 March, ESA SP-473, 2001, pp. 501–506. 2001.
[13] R. O'Hara, N. Johnson, Re-entry survivability risk assessment of the extreme ultraviolet explorer, Orbital Debris Q. News 6 (2) (2001) 8 April.
[14] R. Smith, K. Bledsoe, J. Dobarco-Otero, Reentry Survivability Analysis of the Hubble Space Telescope (HST), The Orbital Debris Quarterly News 8 (4) (2004) 3 October.
[15] W. Rochelle, R. O'Hara, Reentry survivability analysis of the earth observing system (EOS)-aura spacecraft, Orbital Debris Q. News 7 (1) (2002) 12–13 January.
[16] R.L. Kelley, Reentry survivability analysis of the global precipitation measurement spacecraft, Orbital Debris Q. News 13 (3) (2009) 3–4 July.
[17] R. Smith, J. Dobarco-Otero, W. Rochelle, Reentry survivability analysis of gamma-ray large area space telescope (GLAST) satellite, Orbital Debris Q. News 8 (2) (April 2004) 6.
[18] T. Lips, Destructive re-entry analysis of GOCE with SCARAB, HTG-Report-05-07, Hyperschall Technologie Göttingen, Katlenburg-Lindau, Germany, 29 November 2005.
[19] W.H. Ailor, Large Constellation Disposal Hazards, Center for Space Policy and Strategy, The Aerospace Corporation, El Segundo (CA), USA, January 2020.
[20] Anonymous, PAM-D, Debris falls in Saudi Arabia, Orbital Debris Q. News 6 (2) (2001) 1 April.
[21] R.L. Kelley, N.M. Hill, W.C. Rochelle, N.L. Johnson, T. Lips, Comparison of ORSAT and SCARAB Reentry Analysis Tools for a Generic Satellite Test Case, 38th COSPAR Scientific Assembly, PEDAS1-0021-10, Bremen, Germany, 2010 18-25 July.
[22] R. Smith, R. Delaune, J. Dobarco-Otero, Reentry survivability analysis of the terra satellite, Orbital Debris Q. News 9 (4) (2005) 3–4 October.
[23] R. Smith, J. Dobarco-Otero, J. Marichalar, W. Rochelle, Reentry survivability analysis of the tropical measuring mission (TRMM) Spacecraft, Orbital Debris Q. News 8 (1) (2004) 4–5 January.
[24] W.C. Rochelle, J.J. Marichalar, Reentry survivability analysis of the upper atmosphere research satellite (UARS), Orbital Debris Q. News 7 (2) (2002) 2–3 April.
[25] JAXA, JAXA-CAA-109029 Manual for *Re*-entry Survivability Analysis. Tsukuba, Japan, 2016.
[26] Current world population. https://www.worldometers.info/world-population/, 2021 (accessed 15 July 2021).
[27] L. Anselmo, C. Pardini, The management of the mir reentry in Italy, in: Proceedings of the International Workshop on Mir Deorbit, ESA SP-498, European Space Agency, Darmstadt, Germany, 2002, pp. 83–90.
[28] U.S. Government, Orbital Debris Mitigation Standard Practices, November 2019 update.
[29] Range commanders council range safety group risk committee, common risk criteria for national test rangesRCC 321-16, U.S. Army White Sands Missile Range, New Mexico, USA, 2016.
[30] W.H. Ailor, Hazards of reentry disposal of satellites from large constellations, J. Space Safety Eng. 6 (2019) 113–121, doi:10.1016/j.jsse.2019.06.005.